

**CORRELATION BETWEEN PHOTOELECTROCHEMICAL BEHAVIOUR AND  
PHOTOCATALYTIC ACTIVITY AND SCALING-UP OF P25-TiO<sub>2</sub>  
ELECTRODES.**

Cristina Pablos<sup>1</sup>, Javier Marugán<sup>1,\*</sup>, Rafael van Grieken<sup>1</sup>, Cristina Adán<sup>1</sup>, Ainhoa Riquelme<sup>1</sup>  
and Jesús Palma<sup>2</sup>.

<sup>1</sup> Department of Chemical and Environmental Technology, ESCET, Universidad Rey Juan Carlos, C/ Tulipán s/n, 28933 Móstoles (Madrid), Spain.

\* Tel: +34 91 488 7007, Fax +34 91 488 7068, E-mail: javier.marugan@urjc.es

<sup>2</sup> Instituto IMDEA Energía, c/ Tulipán s/n, 28933, Madrid, Spain

Published on  
Electrochimica Acta 130 (2014) 261–270.  
[doi:10.1016/j.electacta.2014.03.038](https://doi.org/10.1016/j.electacta.2014.03.038)

## **ABSTRACT**

The use of TiO<sub>2</sub> electrodes may solve the two main drawbacks of photocatalytic processes: i) the necessity of recovering the catalyst and ii) the low quantum yield in the use of the radiation. This work focuses on the correlation between the photoelectrochemical properties of TiO<sub>2</sub> electrodes and their activity for the photoelectrocatalytic oxidation of methanol. Particulate TiO<sub>2</sub> electrodes prepared by deposition of P25-TiO<sub>2</sub> nanoparticles on titanium (TiO<sub>2</sub>/Ti) or conductive glass support (TiO<sub>2</sub>/ITO) seem to be effective for charge carrier transference on TiO<sub>2</sub> surface favouring the formation of ·OH radicals and consequently, the oxidation of molecules. In contrast, thermal TiO<sub>2</sub> electrodes prepared by annealing of titanium (Ti) present better properties for charge carrier separation as a consequence of the application of a potential bias. Despite reducing charge carrier recombination by applying an electric potential bias, the activity of thermal electrodes remains lower than that of P25-particulate electrodes. TiO<sub>2</sub> structure of P25-particulate electrodes does not completely allow developing a potential gradient. However, their adequate TiO<sub>2</sub> layer characteristics for charge carrier transfer lead to a reduction in charge carrier recombination making up for the lack of charge carrier separation when applying an electric potential bias. TiO<sub>2</sub>/Ti showed the highest values of activity. Therefore, the combination of the suitable TiO<sub>2</sub> surface properties for charge carrier transfer with an adequate conductive support seems to increase the properties of the electrode for allowing charge carrier separation. The scaling-up calculations for a TiO<sub>2</sub>/ITO electrode do lead to good estimations of the activity and photocurrent of larger electrodes since this photoanode made from ITO as conductive support does not seem to be significantly affected by the applied potential bias.

**KEYWORDS:** particulate electrode; photoelectrocatalysis; thermal electrode; TiO<sub>2</sub>; scaling-up

## **1. INTRODUCTION**

Advanced Oxidation Processes (AOPs) have been long studied for the treatment of wastewater [1]. Among them, TiO<sub>2</sub> heterogeneous photocatalysis, based on the generation of hydroxyl radicals upon irradiation of the catalyst with UVA light, has shown to be really effective for the degradation of many chemical pollutants [2]. This technology provides some advantages over other AOPs such as working under ambient conditions of temperature and pressure, and without additional chemical reagents. However, it has several drawbacks that hinder its massive commercialization, mainly due to the required separation of the catalyst after the treatment and the low quantum efficiency in the use of the absorbed radiation for hydroxyl radical generation due to the recombination of the photogenerated charge carriers on the semiconductor particles. One of the proposed solutions for both problems is the immobilisation of TiO<sub>2</sub> onto a conductive support and the application of a small potential bias between this photocatalytic electrode and a counter electrode. Under illumination, the holes migrate to the semiconductor-electrolyte interface where the water oxidation occurs, producing hydroxyl radicals, and the electrons are led to the back of the conductive support by the positive potential towards the cathode where the oxygen reduction takes place. The spatial separation of both reactions reduces the charge-carrier recombination, increasing the quantum efficiency of the process.

This *Electric Field Enhancement* (EFE) has been reported to improve the photocatalytic efficiency for degradation of organic pollutants. Since the first results reported by Vinodgopal et al. [3] and Kim and Anderson [4], several research groups have reported increasing efficiencies in the photoelectrocatalytic oxidation of several organic compounds [5]. However, some aspects of the application of photoelectrocatalytic processes for water

treatment purposes remain still unclarified. Firstly, the efficiency of the photoelectrocatalytic processes is quite dependent on the electrode type (conductive material and TiO<sub>2</sub> structure) [6,7]. Thus, the efficiency of each photoelectrode might be different depending on the kind of pollutant to be removed. Secondly, oxidation activity given by a photoelectrode has been usually extrapolated from the photocurrent or electron flow registered from the anode to the cathode during the photoelectrochemical characterization of the photoelectrodes; although some authors have reported certain discrepancies in that correlation [8]. Finally, possible commercial applications requires carrying out the scaling-up of photoelectrodes to be used in a photoelectrocatalytic reactor instead of in a small electrochemical cell, where the photoelectrochemical behaviour of the photoelectrodes is usually studied. Some authors have pointed out the differences observed in efficiency or parameters such as potential bias that should be modified when photoelectrodes are scaled up [7,9].

Therefore, the aim of this work is to investigate the correlation between the electrochemical characterization of different TiO<sub>2</sub> electrodes and their photoelectrocatalytic activity, evaluating if the ratio between the photocurrent and photoelectrocatalytic activity of photoelectrodes is kept constant after being scaled up.

## 2. EXPERIMENTAL

Photoelectrocatalytic experiments were carried out in the stirred three-electrode electrochemical cell whose diameter corresponds to 8.5 cm. Three different 5x5 cm TiO<sub>2</sub> working electrodes (WE) were prepared: a thermal TiO<sub>2</sub>/Ti electrode prepared by annealing a titanium foil with a resistance of  $1.1 \cdot 10^{-3} \Omega \text{ sq}^{-1}$  (Goodfellow) at 700°C for 30 min following a

heating rate of  $50^{\circ}\text{C min}^{-1}$  (sample identified as Ti) and two P25-particulate  $\text{TiO}_2$  electrodes prepared by dip-coating in a suspension of AEROXIDE®  $\text{TiO}_2$  P25 (Evonik Industries AG) on different conductive supports, such as titanium foil (samples identified as  $\text{TiO}_2/\text{Ti}$ ) and conductive glass (coated with Indium Tin Oxide, ITO) with a resistance of  $10 \Omega \text{ sq}^{-1}$  (Diamond coatings) (samples identified as  $\text{TiO}_2/\text{ITO}$ ). Both types of dip-coated samples were annealed at  $450^{\circ}\text{C}$  for 120 min following a heating rate of  $5^{\circ}\text{C min}^{-1}$ . This process was repeated up to three times if not otherwise stated. More details of the dip-coating procedure can be found elsewhere [10]. Electrical contact to the conductive support was made by the attachment of a titanium wire using silver conductive epoxy resin and insulation with epoxy resin glue. A nickel mesh (55 % open area) (Goodfellow), placed 1 cm over the working electrode, was used as the counter electrode (CE), being both electrodes placed on a specially designed PTFE cassette. Experiments were carried out using a total working volume of 0.4 L under stirring. The WE received front illumination by four Philips TL 6W black light lamps with a maximum emission peak centred at 365 nm. The UV-A incident photon flow, determined by ferrioxalate actinometry, was  $2.9 \times 10^{-7} \text{ Einstein s}^{-1}$  ( $0.70 \text{ W m}^{-2}$ ). Electrochemical characterization was carried out by cyclic voltammetry (CV) at a sweep rate of  $50 \text{ mV s}^{-1}$ , once verified that differences in the results obtained at this sweep rate are negligible in comparison with those recorded at lower values of  $10 \text{ mV s}^{-1}$ . Amperometric measurements were recorded during the photoelectrocatalytic reactions at +1 V of potential bias, if not otherwise specified, using an Eco-Chemie μAutolab Type III potentiostat and a Ag/AgCl reference electrode (Bas Inc.). A two-electrode configuration of the cell (without reference electrode) was also used for scaling-up calculations. The recorded photocurrents values were transformed into photocurrent densities by considering the irradiated or photoactive surface of the electrodes ( $25 \text{ cm}^2$ ).

$\text{TiO}_2/\text{ITO}$  electrodes were scaled up to a cylindrical two-electrode photocatalytic reactor (Figure 2), which consists of an annular reactor 15 cm long, 3 cm inner-tube diameter and 5 cm external-tube diameter operating in a closed recirculating circuit driven by a centrifugal pump, with a stirred reservoir tank. Experiments were carried out using a total working volume of 1 L.  $\text{TiO}_2/\text{ITO}$  electrodes whose geometric area correspond to  $141.4 \text{ cm}^2$  where placed as the inner-tube. Insulated Cu wire was glued onto both extremes of the photoelectrode as detailed above. The counter electrode was a nickel mesh placed surrounding and facing the working electrode. Both electrodes were kept separated a distance of 0.5 cm by Teflon® spacers attached to the external-tube by epoxy resin glue. The illumination, provided by a Philips TL 6W black light lamp placed in the axis of the reactor, came from the backside of the WE. The UV-A incident photon flow, determined by ferrioxalate actinometry, was  $1.0 \times 10^{-6} \text{ Einstein s}^{-1}$  ( $0.47 \text{ W m}^{-2}$ ). A potential bias was applied using as power supply the same potentiostat described above in a two-electrode configuration.

Methanol was chosen as model chemical pollutant to carry out one-hour experiments of photoelectrocatalytic degradation at initial concentrations of 0.01, 0.1 and 1 M, using 0.1 M  $\text{Na}_2\text{SO}_4$  as supporting electrolyte. The evolution of the reaction was followed through the colorimetric determination of the formaldehyde produced along the reaction following the Nash's method [11]. Despite Villareal et al. [12] suggested that the final product of the oxidation of methanol corresponds to  $\text{CO}_2$ , being formaldehyde one of the intermediates, according to Sun and Bolton [13], the presence of methanol in excess leads to a quantitative production of formaldehyde.

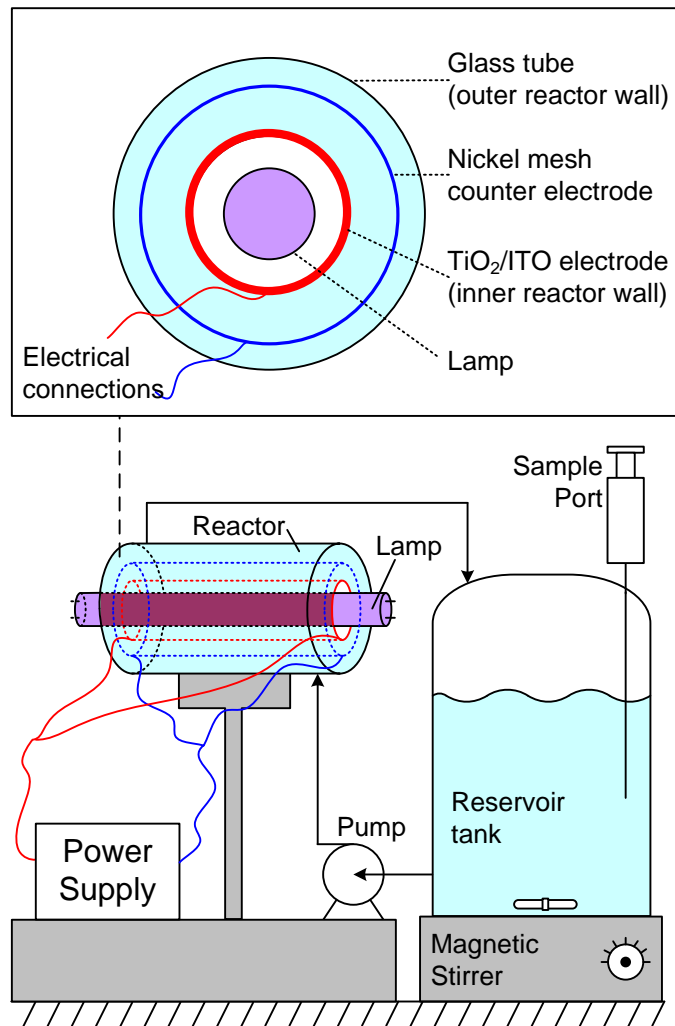


**Figure 1.** Schematic representation of the experimental photoelectrocatalytic reactor (see text for details).

X-ray diffractograms of the 25 cm<sup>2</sup>-area electrodes were measured at room temperature using an X-ray diffractometer (Philips, X'PERT MPD, Cu K $\alpha$  radiation). Scanning electron microscopy (SEM) micrographs were taken on a JEOL JSM-6400 working at an acceleration voltage of 15–30 kV. UV-vis absorption spectra of the electrodes were recorded in the 350–500 nm range with a Varian Cary 500 Scan UV–VIS–NIR spectrophotometer operating in the transmission mode.

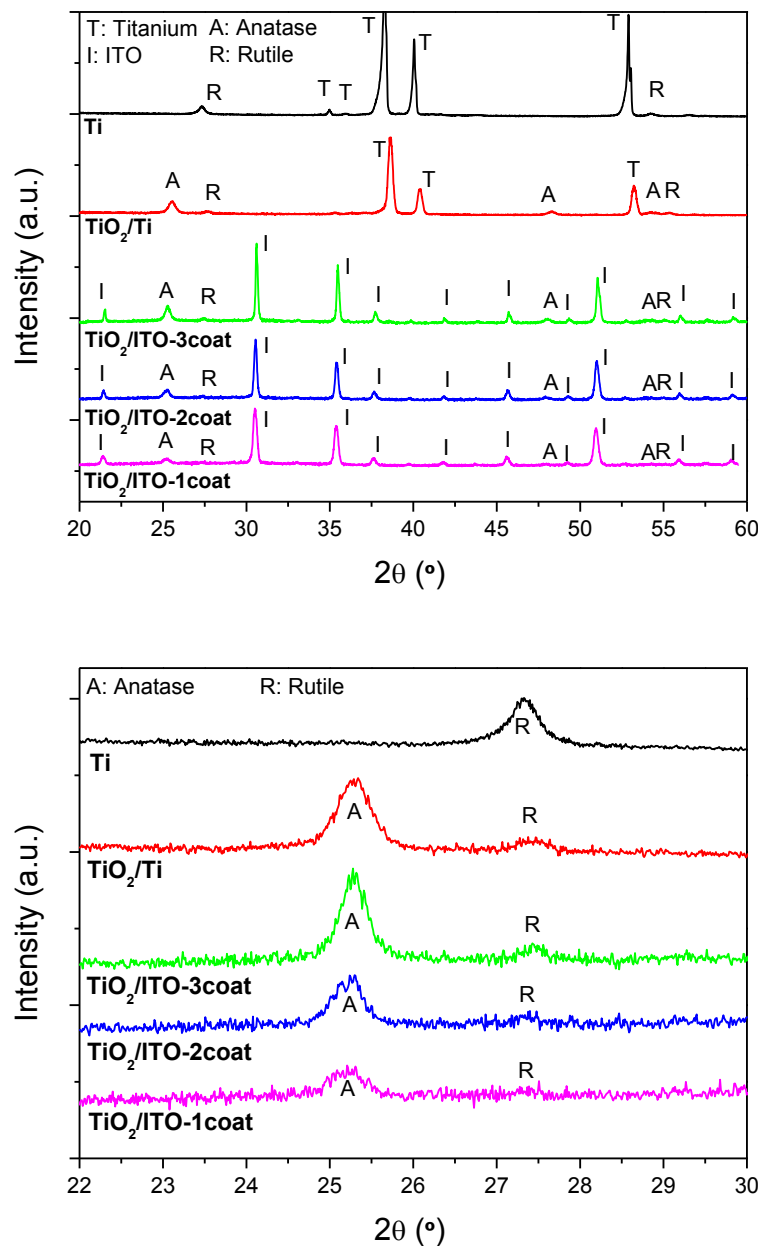
### **3. RESULTS AND DISCUSSION**

#### **3.1. Structural characterization of TiO<sub>2</sub> photoelectrodes.**

Figure 2 shows the X-ray diffractograms of five different TiO<sub>2</sub> electrodes. As seen, P25-particulate electrodes maintained the anatase and rutile signals characteristic of the well-known composition of P25 TiO<sub>2</sub> after the thermal treatment, with both anatase and rutile peaks more intense as the number of coating cycles increases. In contrast, thermal electrodes prepared by annealing of metal titanium consisted always of rutile as single TiO<sub>2</sub> phase, independently of the temperature of the treatment (in the range from 400 to 700°C, data not shown).

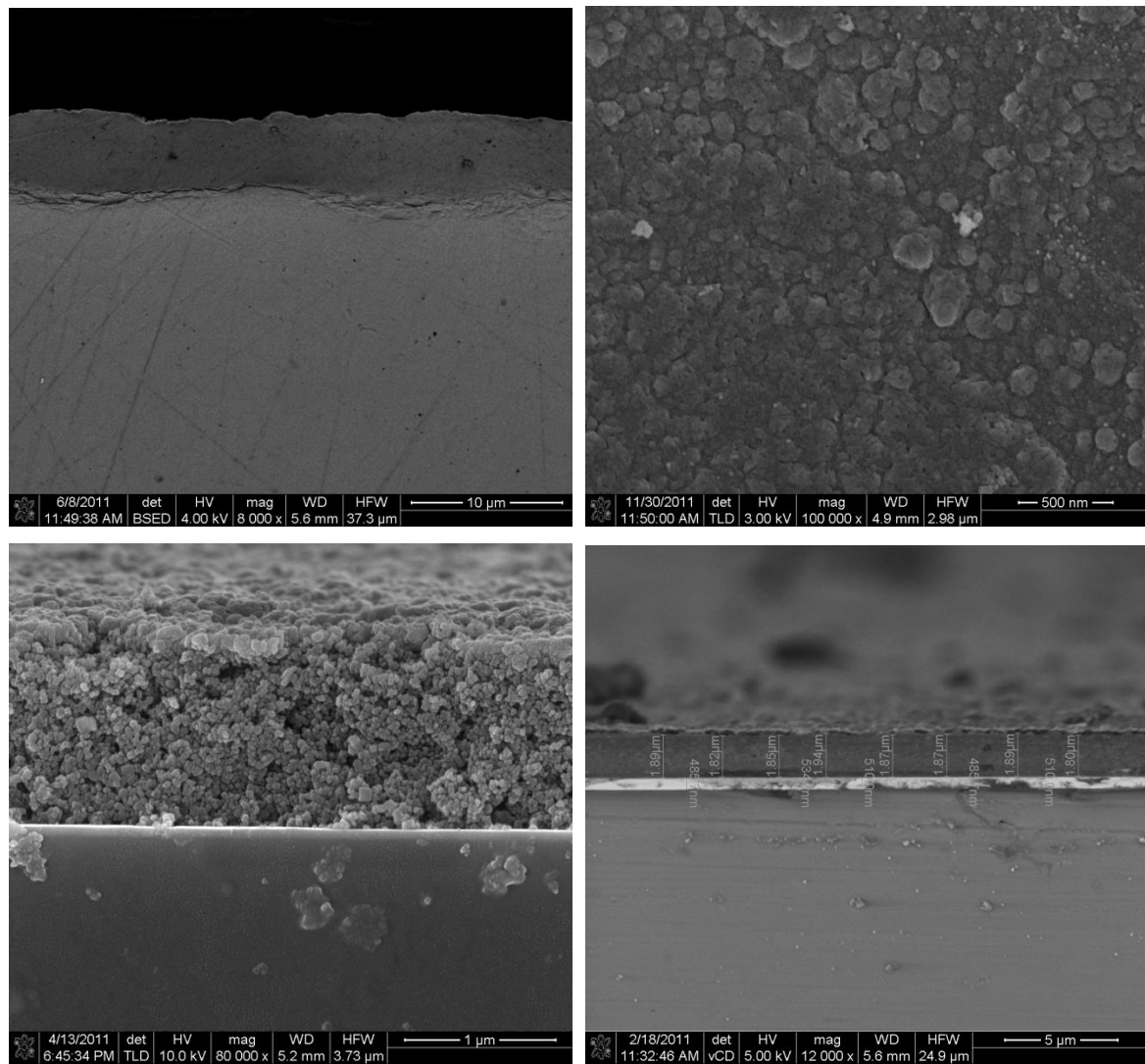
Figure 3 shows surface and cross sections of the thermal electrode (Ti) and the P25-particulate electrode TiO<sub>2</sub>/ITO. It must be noticed that no significant differences in surface have been observed between both P25-particulate electrodes. Cross sections (left) show that TiO<sub>2</sub> layer for Ti electrode, thermally formed at 700°C, has merged into the titanium foil. In contrast, the formed particulate TiO<sub>2</sub> layer for P25-particulate electrodes has been set down onto the conductive substrate, leading to a clear limit between both materials that could introduce a significant resistance for electron transport from TiO<sub>2</sub> layer to the conductive support. Concerning to the surface, there are also differences between thermal and P25-particulate electrodes. P25-particulate electrodes show a highly porous TiO<sub>2</sub> layer formed by aggregates made of the nm-sized particles that constitute P25 TiO<sub>2</sub>. On the contrary, thermal TiO<sub>2</sub> layer is much more dense and consequently, less porous. This fact leads to a lower active surface of TiO<sub>2</sub> in contact with the electrolyte for the thermal electrode in comparison with that of P25-particulate electrodes, which could limit the charge carrier transference on

TiO<sub>2</sub> surface, reducing efficiency for the oxidation of pollutants.



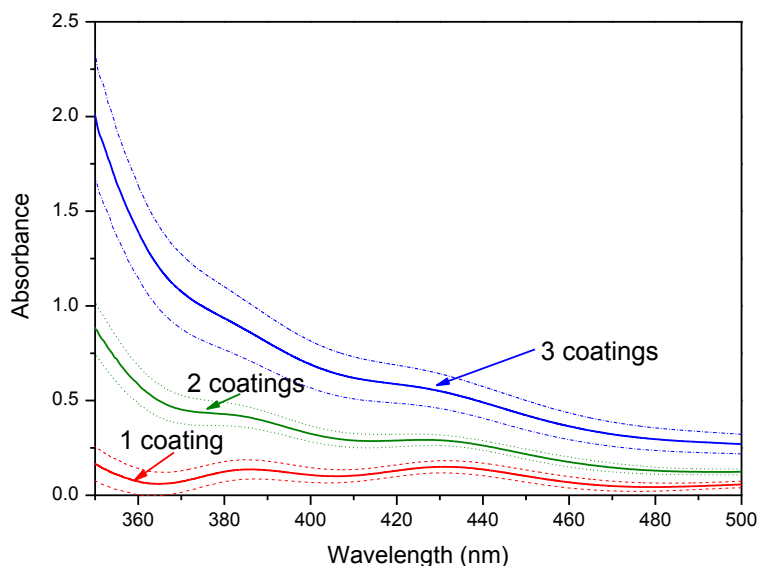
**Figure 2.** XRD patterns of the thermal electrode (Ti) and the P25-particulate electrodes using titanium support ( $\text{TiO}_2/\text{Ti}$ ) and ITO glass support with increasing number of coatings ( $\text{TiO}_2/\text{ITO}$ ) detailing the main diffraction signals of anatase and rutile.

Figure 3 also shows a SEM micrograph of cross section of a TiO<sub>2</sub>/ITO photoelectrode with 3 coating cycles. The three layers of the constituent materials of the TiO<sub>2</sub>/ITO photoelectrodes are observed: glass support, ITO layer and P25-particulate TiO<sub>2</sub> layer. It was observed an increase in the thickness of the TiO<sub>2</sub> layer when repeating a new TiO<sub>2</sub> coating cycle (data not shown). The values of average thickness of the TiO<sub>2</sub> layer for each TiO<sub>2</sub>/ITO photoelectrode correspond to  $0.34 \pm 0.05$ ,  $0.88 \pm 0.12$  and  $1.87 \pm 0.40$   $\mu\text{m}$  for 1, 2 and 3 coatings, respectively.



**Figure 3.** SEM micrographs of cross (left) and top (right) section of TiO<sub>2</sub> for the Ti thermal electrode (top). Cross sections of a TiO<sub>2</sub>/ITO P25-particulate electrode after 3 coating cycles (bottom).

The increase in the thickness of the TiO<sub>2</sub> layer leads to a higher UV-A absorption as the number of TiO<sub>2</sub> coating cycles increases, as shown in Figure 4. It must be noticed that 1 coating-TiO<sub>2</sub>/ITO electrode barely absorbs UV-vis radiation, while a noticeable increase is observed for 3 coating-TiO<sub>2</sub>/ITO electrode, corresponding to 10 % of transmittance around 380 nm and only 1 % around 350 nm (absorbance values of 1 and 2, respectively). This increase in radiation absorption would lead to an increase in the photocatalytic activity of the electrodes, being expected the highest for the 3 coating-TiO<sub>2</sub>/ITO electrode. Moreover, as the UV-A absorption is almost total, additional coatings cycles should not lead to a significant increase in the absorption (and therefore in the expected activity).



**Figure 4.** UV-vis absorption spectra of TiO<sub>2</sub>/ITO electrodes with different number of TiO<sub>2</sub> coating cycles. Errors depicted as broken lines have been estimated from different batches of electrodes. Baseline of the spectra calculated with the uncoated ITO glass.

### **3.2. Photoelectrochemical characterization of TiO<sub>2</sub> electrodes.**

Figure 5 shows the photocurrent density ( $I_{ph}$ ) - electric potential ( $E$ ) curves under illumination in 0.1 M Na<sub>2</sub>SO<sub>4</sub> as supporting electrolyte. As expected, it was found that without UV illumination, no measurable current is observed (data not shown).

A linear dependency of the photocurrent density with the applied potential bias is observed for the thermal photoelectrode, in agreement with the classic theory for n-type semiconductors [14]. This linear dependency can be also observed for P25-particulate electrodes at very low potential values, although this fact is still a matter of controversy. Some authors have pointed out an independent relation between photocurrent and electric potential as a consequence of nm-sized particles that form the particulate electrodes, which hinder the development of the depletion layer across the particles, responsible for the charge carrier separation when an electrical potential bias is applied. Thus, the registered photocurrent and consequently the charge carrier transport is attributed to diffusion [9,15-17]. Other mechanisms have been proposed, suggesting that only free electrons released by photohole surface capture reaction are able to migrate under an electric potential bias [18]. Finally, some authors do agree with the formation of a depletion layer for particulate electrodes [8,19,20].

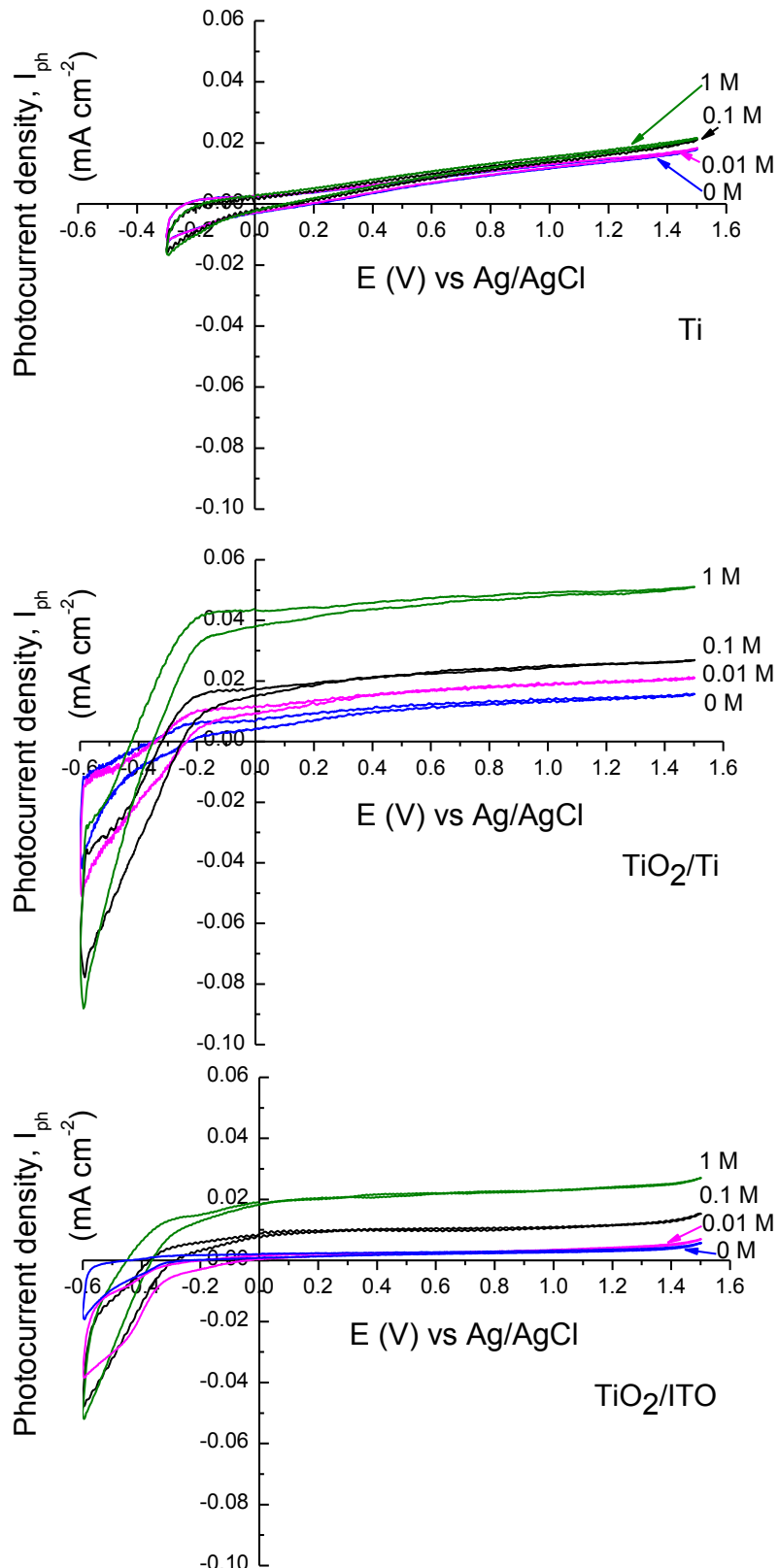


**Figure 5.** Cyclic photovoltammograms (CV) in 0.1 M  $\text{Na}_2\text{SO}_4$  and at different methanol concentrations (0.01, 0.1 and 1 M) in 0.1 M  $\text{Na}_2\text{SO}_4$ , recorded at a sweep rate of 50 mV s<sup>-1</sup> for Ti,  $\text{TiO}_2/\text{Ti}$  and  $\text{TiO}_2/\text{ITO}$  photoelectrodes.

Apart from the linear relation for  $I_{ph}$ - $E$  curves at lower potential bias for P25-particulate electrodes, significant differences are observed in voltammograms between thermal and P25-particulate photoelectrodes, the latter showing saturation in the photocurrent density dependence. According to Jiang et al. [18] and Zhao et al. [21] for particulate electrodes and Leng et al. [22] for anatase-rich electrodes, photocurrent is linearly enhanced as the electric potential increases. This behaviour has been attributed to the electron transport being the determining step of the overall process, up to reaching a plateau for higher potentials where photocurrent is saturated, becoming the diffusion of charge carriers in the semiconductor surface the limiting step of the whole process. According to the plots in Figure 5, the charge carrier transport seems to be the controlling step for the thermal electrodes, since a linear  $I_{ph}$ - $E$  trend is observed for all the range of applied potentials. In contrast, individual  $\text{TiO}_2$  particles in particulate photoelectrodes seems to be too small to form a depletion layer or potential gradient at the electrolyte interface, not leading to a complete band bending across the film, quickly reaching a saturated photocurrent density, in agreement with previous reports [3,6,23].

Other differences in photovoltammograms are observed regarding the potential bias corresponding to the anodic current where the value of photocurrent equals zero (which can be considered as rough approximations to the flat band potential,  $V_{fb}$ ). These values correspond to -0.02, -0.27 and -0.36 V for Ti,  $\text{TiO}_2/\text{Ti}$  and  $\text{TiO}_2/\text{ITO}$  respectively, approximately similar to common values of  $V_{fb}$  reported for n-type semiconductors (from -0.05 to -0.75 V) [3]. The fact that P25-particulate electrodes show more negative values of  $V_{fb}$  than that of the thermal electrode might be related to their anatase-rutile composition, since the flat band potential of anatase (mainly  $\text{TiO}_2$  form for P25-particulate electrodes) has been

reported to be more negative than that of rutile ( $\text{TiO}_2$  form present in the thermal electrode) [23].

As far as the absolute values of the photocurrent density are concerned, the highest  $I_{ph}$  values are observed for Ti and  $\text{TiO}_2/\text{Ti}$  electrodes, showing the  $\text{TiO}_2/\text{ITO}$  photoelectrode the lowest  $I_{ph}$  value at zero methanol concentration and larger applied biases. For the thermal electrode, this fact can possibly be due not only to a better charge carrier separation as a consequence of a more developed potential gradient, but also to a higher conductivity of the  $\text{TiO}_2$  layer [9,24]. It would lead to a lower resistance to the electron transport between the  $\text{TiO}_2$  layer and the support. Moreover, since  $\text{TiO}_2$  layer grows in intimate contact with the conductive titanium substrate, it would also reduce the resistance to electron transport through the layer. In addition to that, since  $\text{TiO}_2$  layer is not porous, no oxygen would be present inside the layer, not being able to act as an electron scavenger [15].  $\text{TiO}_2/\text{Ti}$  does not seem to have a developed depletion layer since it has shown a typical  $I_{ph}-E$  curve for a particulate electrode (linear behaviour  $I_{ph}-E$  reaching a saturated photocurrent density for lower electric potential values compared to thermal electrodes). However, similar photocurrent density values are observed for  $\text{TiO}_2/\text{Ti}$  compared to those of the thermal Ti electrode in absence of organics and larger applied biases. In fact, these values are really high compared to those of  $\text{TiO}_2/\text{ITO}$ , the other P25-particulate electrode. Thus, the reason might be due to the conductive support. This aspect has been pointed out as really important by several groups [15,18]. Since a titanium support presents more conductivity than that of ITO, it might favour the electron transport from  $\text{TiO}_2$  to the conductive support. It is in agreement with other authors who have also reported better results for titanium supports than those of ITO [20,25]. Therefore, several factors such as anatase-rutile composition,  $\text{TiO}_2$  structure and  $\text{TiO}_2$ -conductive support interaction seem to have influence on the charge carrier separation.

The effect of the addition of organic compounds such as methanol in the photovoltammograms is also depicted in Figure 5, using different methanol concentrations corresponding to 0.01, 0.1, and 1 M. The presence of methanol does not substantially affect the behaviour of Ti electrode. In contrast, the photocurrent density values rise for both P25-particulate electrodes as methanol concentration increases, in agreement with other authors [6,7,18,23]. It must be noted that  $\text{TiO}_2/\text{ITO}$  electrode reach the same  $I_{ph}$  values in the presence of methanol as those of the thermal Ti electrode, whereas photocurrent density values reached by  $\text{TiO}_2/\text{Ti}$  are even higher. The most accepted oxidation mechanism for methanol is their photooxidation to formaldehyde through hydroxyl radicals rather than through a direct hole transfer mechanism [26]. Since particulate electrodes (anatase-rich) are supposed to be more efficient to oxidize methanol than the thermal electrode (pure rutile), some authors have associated the increase in  $I_{ph}$  values in presence of methanol for particulate electrodes as a consequence of the electron injection in the conduction band released by intermediate compounds [27], leading to a so-called current doubling effect. However, the increase in  $I_{ph}$  values when adding 1 M methanol for  $\text{TiO}_2/\text{Ti}$  and  $\text{TiO}_2/\text{ITO}$  is more than twice compared to those of pure electrolyte. Therefore, the increase in  $I_{ph}$  values in presence of methanol only for P25-particulate electrodes might be due to another mechanism [9,15], such a reduction in recombination of charge carriers on  $\text{TiO}_2$  surface. It would be probably due to a higher interface electrolyte for P25-particulate electrodes as a consequence of their high porosity and therefore, high surface area as well. An improvement in charge carrier transference might also enhance the potential gradient across  $\text{TiO}_2$  particles, leading to a shift in the flat band potential to more negative values in presence of methanol as shown in Figure 5 and suggested by Jiang et al. [18].

Therefore, P25-particulate electrodes seem to present better properties for charge carrier transfer on TiO<sub>2</sub> surface favouring the oxidation of pollutants, while the thermal electrode shows better properties for charge carrier separation under the application of an electric potential bias. Both phenomena lead to a reduction in the charge carrier recombination, being the next step of this research the evaluation of their impact on the photocatalytic and photoelectrocatalytic activity of these electrodes.

Figure 6 shows the photovoltammograms obtained for TiO<sub>2</sub>/ITO electrodes in pure electrolyte and by adding methanol 0.1 M when increasing the number of coatings and consequently the TiO<sub>2</sub> layer thickness. In pure electrolyte, in the absence of organics, the increase in the layer thickness does not seem to increase the photoelectrochemical response. Although the thickness of TiO<sub>2</sub> layer corresponding to 2 and 3-coating TiO<sub>2</sub>/ITO electrodes have shown to possess the most suitable properties for UV-A absorption, the thickness of TiO<sub>2</sub> layer might have a strong influence in the charge carrier separation. Since the distance to be crossed by electrons up to reaching the conductive support (ITO) increases as thickness layer increases, electrons can readily be lost through TiO<sub>2</sub> layer. This fact would explain not having observed the expected increased in photocurrent density values for 2 and 3-coating electrodes. It is in agreement with other authors who have also reported that thick TiO<sub>2</sub> layers might hinder electron transport up to the conductive support [17,22,28-32].

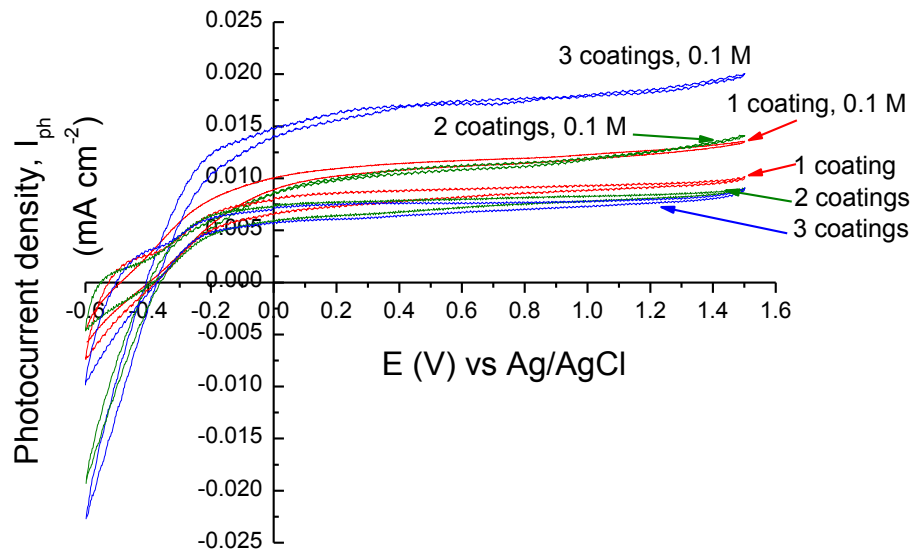


**Figure 6.** Cyclic photovoltammograms (CV) in 0.1 M  $\text{Na}_2\text{SO}_4$  and methanol 0.1 M in 0.1 M  $\text{Na}_2\text{SO}_4$ , recorded at a sweep rate of 50 mV s<sup>-1</sup> for  $\text{TiO}_2/\text{ITO}$  photoelectrodes with different number of coating cycles.

In contrast, the presence of methanol increases the photochemical response of the electrodes, especially for that with the thickest  $\text{TiO}_2$  layer. As explained above, charge carrier transfer at  $\text{TiO}_2$ -electrolyte interface leads to a reduction between charge carriers which might enhance the potential gradient in comparison with no addition of organic compounds. Thicker  $\text{TiO}_2$  layers present higher absorption of UV-A radiation and higher surface area in contact with the electrolyte and consequently with methanol. Hole transfer would be favoured for those electrodes and as a consequence the development of the depletion layer. Thus, electron transport resistance due to the thickness of the  $\text{TiO}_2$  layer does not become so crucial for the whole process.

### **3.3. Photocatalytic (PC) and photoelectrocatalytic (PEC) evaluation of TiO<sub>2</sub> electrodes.**

#### *3.3.1. Effect of potential bias.*

The photocatalytic oxidation of methanol leads to the formation of formaldehyde with an almost total selectivity [26]. The kinetics of the process, considering the excess of methanol present in solution can be successfully described by a zero-order kinetic model. Figure 7 shows the influence of increasing the electric potential bias applied on the values of the surface zero-order kinetic constant ( $k$ ) for formaldehyde production due to methanol oxidation being its initial concentration 0.1 M (top). Figure 7 also shows the correlation of these  $k$  values with values of photocurrent measured by amperometry through the photoelectrocatalytic experiments (bottom).

The application of an electric potential bias significantly improves the efficiency in the photocatalytic oxidation of methanol when using a thermal electrode confirming the suitable properties of this photoelectrode for allowing charge carrier separation, reducing charge carrier recombination. In contrast, P25-particulate electrodes do not show such an increase in the efficiency when applying an electric potential bias. This could be due to the fact that they do not completely develop a depletion layer, as discussed above, being in agreement with the photoelectrochemical characterization data, making their behaviour almost independent on the applied potential bias. It must be noticed that although the thermal electrode shows better properties for charge carrier separation in comparison with those of P25-particulate electrodes, the values of  $k$  for Ti electrode are really low compared to those of TiO<sub>2</sub>/Ti and TiO<sub>2</sub>/ITO. In contrast, P25-particulate electrodes seem to show suitable properties for favouring charge carrier transfer on TiO<sub>2</sub> surface since they present a high surface in contact

with the electrolyte, leading to a higher photocatalytic activity.

Concerning the comparison between both P25-particulate electrodes, TiO<sub>2</sub>/Ti photoelectrode seems to be more effective. It may be explained by the slight improvement in the charge carrier separation, which might be derived of the higher conductivity of titanium support compared to that of ITO glass, facilitating the electron transport from TiO<sub>2</sub> layer to the external circuit and thus preventing charge carrier recombination. Other groups [16, 19] have also remarked the importance of the conductivity of the support for particulate electrodes. He et al. [20] reported that titanium is a better support for photoelectrocatalytic applications and Li et al. [25] also stated a bad electron transfer between TiO<sub>2</sub> layer and ITO when using as conductive support. Gan et al. [33] also highlighted the necessity of improving the conductivity of TiO<sub>2</sub> layer to enhance the electron movement from TiO<sub>2</sub> layer to the conductive support. In fact, Li et al. [34] and He et al. [35] included Au and Pt respectively for improving the drift of electrons from TiO<sub>2</sub> layer towards the conductive support made of ITO.

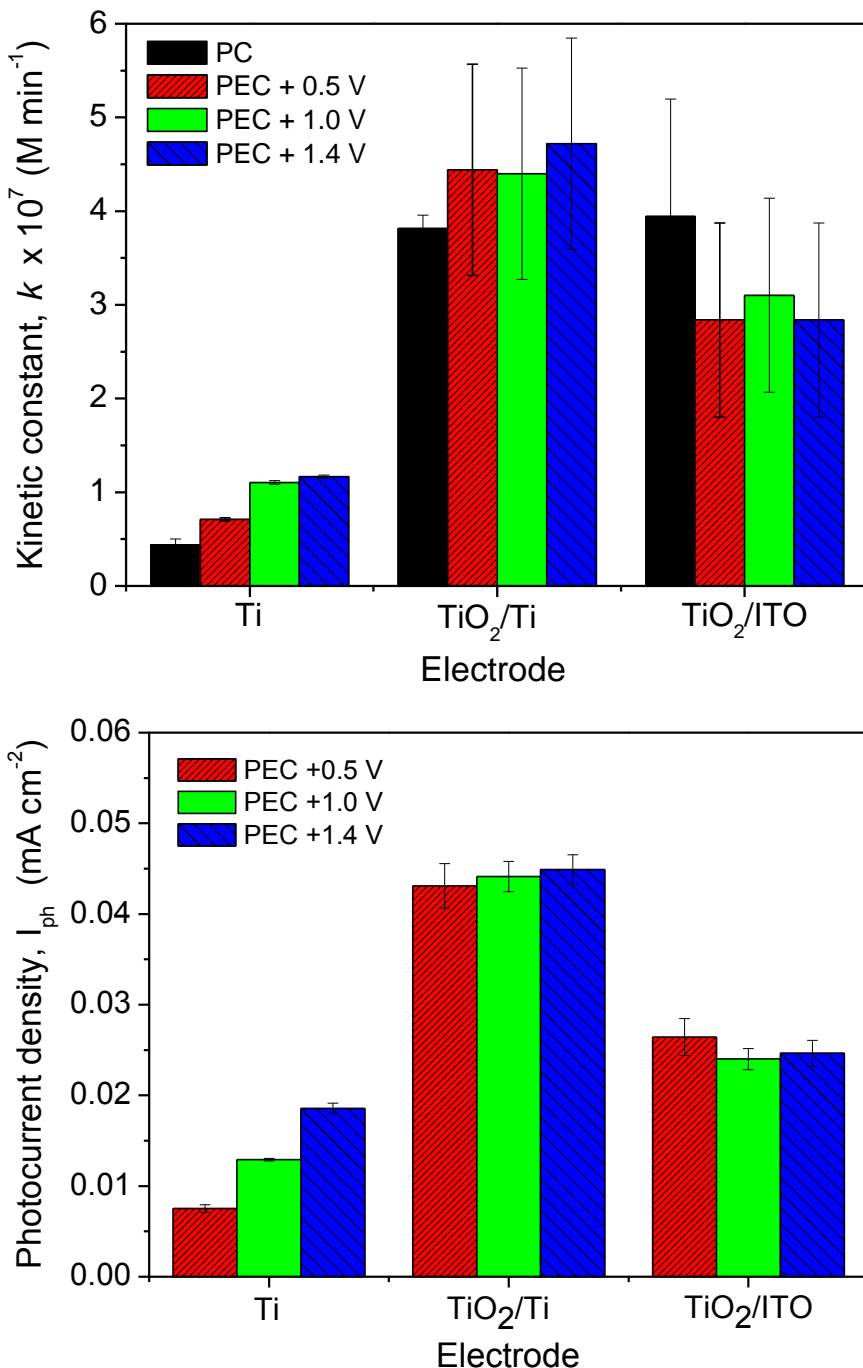


**Figure 7.** Effect of the electric potential bias applied (+0.5, +1.0, and +1.4 V) on methanol oxidation (by measuring the formaldehyde production rate) (top) and photocurrent density. Photocurrent measured by amperometry through the photoelectrocatalytic (PEC) experiments (bottom) for different electrodes. Initial concentration of methanol: 0.1 M.

As expected from the photoelectrochemical characterization, P25-particulate electrodes do not show any enhancement either in values of kinetic constant or in values of photocurrent density by increasing the potential bias from +0.5 to +1.4 V. As shown in photovoltammograms depicted in Figure 5, the saturated photocurrent density is reached when applying an electric potential value of about 0 V, which means that electron transport does not control the photoelectrocatalytic process for higher values of electric potential, and consequently, no increase in formaldehyde formation rate is expected. In contrast, values of kinetic constant for formaldehyde production for the thermal electrode increase as the electric potential bias rises up to values of about +1 V as expected according to its photovoltammograms shown in Figure 5. In this case, electron transport is still the controlling step of the overall process for high electric potential bias, which means that charge carrier separation takes place for the whole range of applied electric potential bias.

Concerning photocurrent measurements, they seem to correspond qualitatively with the trends observed for  $k$  for P25-particulate electrodes. However, a higher value of  $k$  would have been expected when applying an electric potential bias of +1.4 V to the thermal electrode, according to the photocurrent density data. In addition, the increase in photocurrent density values is quite high compared to those of the kinetic constant. When comparing both P25-particulate electrodes, although  $\text{TiO}_2/\text{Ti}$  shows much higher values of photocurrent density, the values of the kinetics constant do not keep that proportion. Consequently it cannot be said that the ratio between the kinetic constant and the measured photocurrent density is constant.

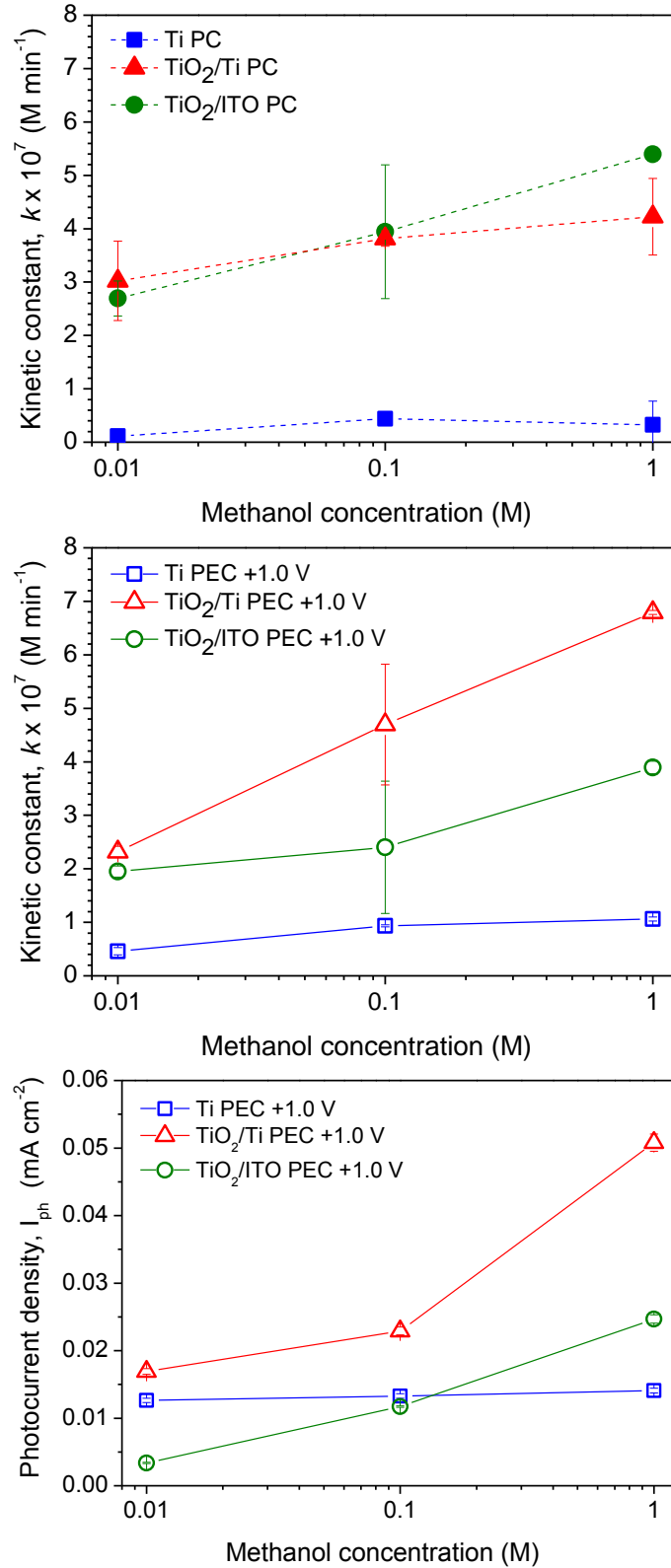
### *3.3.2. Effect of methanol concentration.*

Figure 8 shows the effect of the initial concentration of methanol on the efficiency of the photocatalytic and photoelectrocatalytic oxidation of methanol in terms of values of kinetic constant for formaldehyde production ( $k$ ) for P25-particulate and thermal electrodes. Low values of  $k$  at all tested initial concentrations are observed for the thermal electrode while higher  $k$  values are observed for both P25-particulate electrodes. In addition, values of  $k$  hardly change as initial concentration of methanol increases for the thermal electrode while values of  $k$  increases when adding higher methanol initial concentrations for P25-particulate electrodes. It might be due to different reasons. Since pure rutile is the  $\text{TiO}_2$  form present in the thermal electrode, its activity to oxidize organic compounds is lower than that of the P25-particulate electrodes made mainly by anatase [22]. It may explain the low values of  $k$  obtained for the oxidation of different concentrations of methanol when using a thermal electrode. In addition, the lack of porosity of the thermal electrode leads to a lower active surface which might reduce its oxidation efficiency and to a faster saturation of its active surface. This fact can be suggested by values of  $k$ , which slightly increases when increasing methanol concentration from 0.01 to 0.1 M for the thermal electrode but keep constant for higher methanol concentrations. Moreover, a poor charge carrier transfer may take place as a consequence of a reduced active surface in contact with the electrolyte, not being values of  $k$  affected by different methanol concentrations.

Differences in  $k$  values for P25-particulate electrodes are also observed.  $\text{TiO}_2/\text{Ti}$  electrode shows higher values of  $k$  than those of  $\text{TiO}_2/\text{ITO}$  electrode, which becoming more noticeable for the highest methanol concentration analyzed. Only when using  $\text{TiO}_2/\text{Ti}$  as photoelectrode and for high methanol concentration, the photocatalytic process seems to be

significantly enhanced when applying a potential bias. Since both electrodes present the same surface properties, their differences might be due to their different conductive support. A support with a high conductivity would more easily be able to favour electron transport between TiO<sub>2</sub> layer and the support, allowing the electrons to leave TiO<sub>2</sub> layer and avoiding their possible recombination if stay in TiO<sub>2</sub> layer. Since the high porosity of P25-particulate electrodes (anatase-rich) leads to a high charge carrier transfer on the electrolyte interface, which increases for high methanol concentrations, the development of the potential gradient would be favoured. Thus, charge carrier separation would also be enhanced by a titanium support rather than an ITO support, allowing electrons easily to leave TiO<sub>2</sub> layer towards the back of the support.

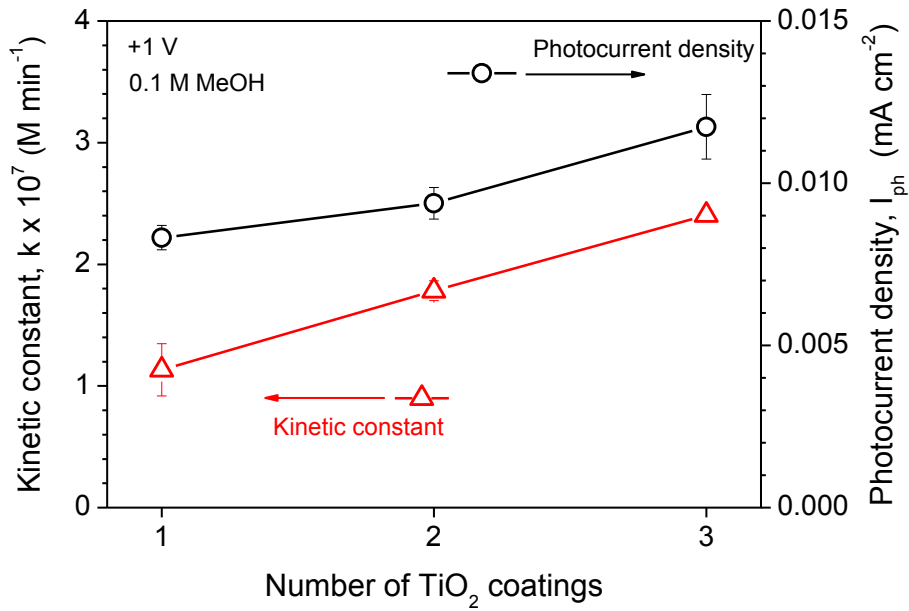
Photocurrent density values show higher differences between both P25-particulate electrodes than they seem to exist according to *k* values. In addition, photocurrent density values measured seem to show a high efficiency of Ti electrode for low methanol concentrations compared to that of TiO<sub>2</sub>/ITO if not paid attention to *k* values. Therefore, photocurrent values do not always correspond with activity in terms of kinetic constant.



**Figure 8.** Effect of methanol concentration on formaldehyde production surface kinetic constant (top) and photocurrent density. Photocurrent measured by amperometry through photoelectrocatalytic experiments (bottom) for different electrodes.

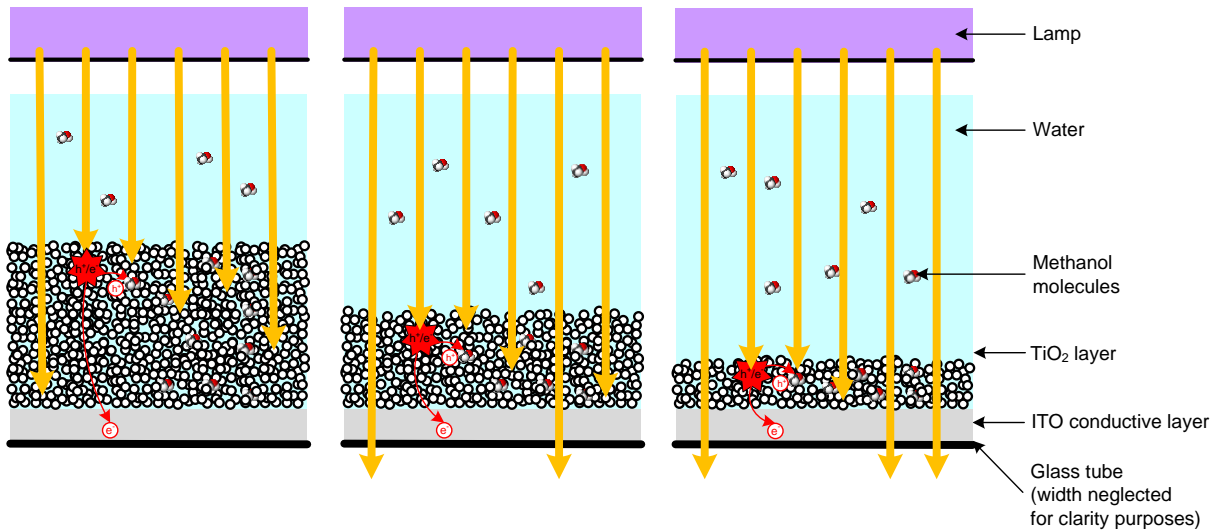
### 3.3.3. Effect of $TiO_2$ layer thickness.

Figure 9 shows the effect of the number of coating cycles of  $TiO_2$ /ITO electrodes on the photoelectrocatalytic oxidation of methanol 0.1 M in terms of the values of kinetic constant for formaldehyde production ( $k$ ). As expected, an increase in the activity is observed as the number of coatings increases. According to the structural and optical characterization data previously discussed, the 3-coating  $TiO_2$ /ITO electrode is expected to give rise to the highest photocatalytic activity since its  $TiO_2$  thickness allows maximizing the absorption of UV-A radiation apart from having a higher surface area for electrolyte interaction. These results are in agreement with those previously reported by Gan et al. [33] and Heikkilä et al. [36] who observed an enhancement of photoelectrocatalytic activity when increasing  $TiO_2$  thickness.



**Figure 9.** Effect of  $TiO_2$  layer thickness on formaldehyde production surface kinetic constant and photocurrent density. Photocurrent measured by amperometry through photoelectrocatalytic experiments for  $TiO_2$ /ITO photoelectrodes with different number of coating cycles.

With regard to photocurrent measurements recorded during the photoelectrocatalytic experiments, also depicted in Figure 9, the relative increase in the values of photocurrent density do not totally correlate with photoelectrocatalytic activities in terms of values of the kinetic constant. Whereas the 3-coating electrode leads to a value of the kinetic constant 2.1 times higher than that of the 1-coating electrode, the photocurrent increase is about 1.45. Therefore, photocurrent measurements only seem to show the influence of  $\text{TiO}_2$  thickness on electron transport. However, photoelectrocatalytic activity should also be checked for taking into account the influence of  $\text{TiO}_2$  thickness on structural and optical properties which are also determining for methanol oxidation. This effect is schematized in Figure 10. As the thickness of the  $\text{TiO}_2$  layer increases, the absorption of radiation does too. However, as the irradiation takes place from the electrolyte side, most of the radiation would be absorbed close to the interphase for thick catalytic films. This fact would favour the charge transfer to the electrolyte but would hinder the electron transport to the back conductive support due to the increase in the distance that the electron has to cross. The net result is that an increase in the thickness should progressively reduce the relative importance of the electrochemically assisted process in comparison with the pure photocatalytic process. Consequently, although qualitatively it can be said that the higher the photoelectrochemical response, the higher the activity, the ratio between both parameters is far from being constant (136.1, 190.0 and 204.8  $\text{M}\cdot\text{min}^{-1}\cdot\text{mA}^{-1}\text{ cm}^2$  for 1, 2 and 3 coatings, respectively). Such significant increase means that the activity of the electrodes cannot be predicted directly from the photoelectrochemical characterization data.



**Figure 10.** Schematic representation of the suggested effect of the increase in TiO<sub>2</sub> thickness on electron transport through the P25-particulate TiO<sub>2</sub> film up to the conductive support.

### 3.4. Scaling-up of TiO<sub>2</sub>/ITO photoelectrodes.

Finally, a comparison between the lab scale reactor and a larger photoelectrocatalytical reactor has been carried out using TiO<sub>2</sub> supported onto ITO substrate. Figure 11 shows a comparison of the photoelectrocatalytic oxidation of methanol 0.1 M using comparable two-electrode configurations in the cell and the photoelectrocatalytic reactor. As photoelectrocatalysis is a surface process and depends on power irradiation as well, the kinetic constant that describes the process and photocurrent values can be divided by the electrode area and irradiation power, allowing the comparison of the activity of electrodes of different sizes. Comparable values of photocurrent density are obtained for both, the cell and the reactor. The surface kinetic constants are also similar for both systems, what means that the surface catalytic response of the electrodes can be scalable under similar values of the irradiation power. Moreover, the different way of illuminating the TiO<sub>2</sub>/ITO photoelectrodes in both systems (from the electrolyte side in the cell and from the back side in the reactor)

does not seem to lead to significant differences in photocurrent density and photoelectrocatalytic methanol oxidation either. Consequently, the existence of ohmic losses in the potential applied that are supposed to appear when photoelectrodes are scaled up [9] do not seem to negatively affect the efficiency of the charge transfer. However, it should be noted that the scaled-up photoelectrodes made from ITO are not positively affected by applied bias evidenced in Figure 7 since no increase in photocurrent density with increasing bias is observed. This may also explain that the values of photocurrent density and kinetic constant obtained for the larger photoelectrode do not seem to be affected by the expected drop in the applied potential bias in the centre of the electrode as a consequence of its scaled-up, which would result in a loss of efficiency of the process.

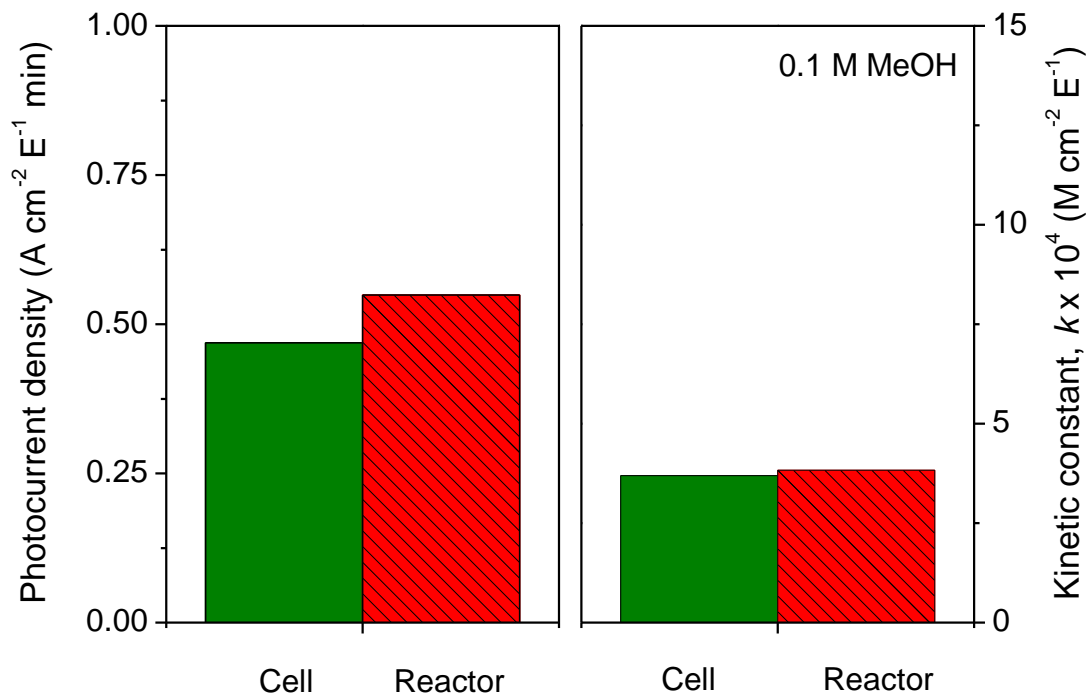


**Figure 11.** Comparison of photocurrent density and formaldehyde production kinetic constant using a  $\text{TiO}_2/\text{ITO}$  photoelectrode in a two-electrode configuration in the cell ( $25 \text{ cm}^2$ , UV-A power irradiation:  $2.9 \times 10^{-7} \text{ Einstein s}^{-1}$ ) and the reactor ( $141.4 \text{ cm}^2$ , UV-A irradiation power:  $1.0 \times 10^{-6} \text{ Einstein s}^{-1}$ ). Initial concentration of methanol: 0.1 M. Potential bias: +1 V.

#### **4. CONCLUSIONS**

Both, charge carrier transfer and charge carrier separation seem to determine the efficiency of a TiO<sub>2</sub> photoelectrode for the photooxidation of organic compounds. Composition and structural characteristics of TiO<sub>2</sub> layer, such as type and size of crystallite form and porosity lead to differences in controlling step of the photoelectrocatalytic process for P25-particulate and thermal electrodes. In addition, TiO<sub>2</sub> and conductive support interaction also seem to be crucial for the photoelectrocatalytic process since it determines electron transport efficiency from TiO<sub>2</sub> layer to the back of the conductive support.

Charge carrier transfer, favoured in P25-particulate electrodes, seems to notably reduce recombination, since these electrodes present a higher photocatalytic and photoelectrocatalytic activity in comparison with that of the thermal electrode. Recombination is reduced for the thermal electrode by charge carrier separation when applying a potential bias, leading to an increase in its photocatalytic activity. However, its lower TiO<sub>2</sub> surface area limits the effectiveness to oxidize organic compounds. TiO<sub>2</sub>/Ti is found to be the most suitable photoelectrode for methanol oxidation. This electrode combine good charge carrier transfer properties derived of its particulate nature together with a reasonable improvement of the charge carrier separation when applying an electric potential bias due to a good interaction between the titanium support and the TiO<sub>2</sub> layer.

It must be noted that from these results it is concluded that if an electrode present good properties for charge carrier separation under an electric potential bias, this fact does not indicate that its photoelectrocatalytic activity for the oxidation of pollutant is better than that of other electrodes, not presenting these properties. In fact, if a photoelectrode does not show adequate properties for charge carrier separation but it does for charge carrier transference,

notably reducing recombination on TiO<sub>2</sub> surface, it can exhibit higher efficiencies for oxidation of pollutants.

TiO<sub>2</sub> thickness is also decisive in photoelectrocatalytic efficiency since it can hinder electron transport across the TiO<sub>2</sub> layer. In fact, the optimum value of TiO<sub>2</sub> thickness for photocatalytic applications cannot be extrapolated for photoelectrocatalytic purposes, as the global effect of this parameter is rather complex, being involved radiation absorption, electron transport and textural properties.

Comparable values of the kinetic constant and photocurrent density have been obtained in the small photoelectrochemical cell and the larger photoelectrocatalytic reactor when they are normalized to the electrode surface area and the incident photon flux of both systems, resulted from the low influence of the applied potential bias on the conductive support of the scaled-up photoelectrode. Consequently, calculations for scaling-up of the studied photoelectrodes could lead to valuable estimations of the activity and photocurrent of larger electrodes from laboratory data.

## **ACKNOWLEDGEMENTS**

The authors gratefully acknowledge the financial support of the Ministerio de Ciencia e Innovación (MICINN) of Spain through the project EMBIOPHOTO (CTM2011-29143-C03-01) and Comunidad de Madrid through the program REMTAVARES (S2009/AMB-1588). Cristina Adán and Cristina Pablos also acknowledge Ministerio de Educación y Ciencia for their Juan de la Cierva contract (JCI-2010-06430), and FPU grant (AP2008-04567), respectively. Thanks also to Fernando Vaquero for his valuable help with some of the experiments.

## REFERENCES

- [1] S. Parsons, Advanced Oxidation Processes for Water and Wastewater Treatment, first ed., IWA Publishing, London, 2004.
- [2] S. Malato, P. Fernández-Ibáñez, M. Maldonado, J. Blanco, W. Gernjak, Decontamination and disinfection of water by solar photocatalysis: recent overview and trends, *Catal. Today* 147 (2009) 1.
- [3] K. Vinodgopal, S. Hotchandani, P. Kamat, Electrochemically assisted photocatalysis. TiO<sub>2</sub> particulate film electrodes for photocatalytic degradation of 4-chlorophenol, *J. Phys. Chem.* 97 (1993) 9040.
- [4] D. Kim, M. Anderson, Photoelectrocatalytic degradation of formic-acid using a porous TiO<sub>2</sub> thin-film electrode, *Environ. Sci. Technol.* 28 (1994) 479.
- [5] T. Egerton, P. Christensen, S. Kosa, B. Onoka, Photoelectrocatalysis by titanium dioxide for water treatment, *Int. J. Environ. Pollut.* 27 (2006) 2.
- [6] P. Christensen, T. Curtis, T. Egerton, S. Kosa, J. Tinlin, Photoelectrocatalytic and photocatalytic disinfection of *E.coli* suspensions, *Appl. Catal. B: Environ.* 41 (2003) 371.
- [7] J. Marugán, P. Christensen, T. Egerton, H. Purnama, Synthesis, characterization and activity of photocatalytic sol–gel TiO<sub>2</sub> powders and electrodes, *Appl. Catal. B: Environ.* 89 (2009) 273.
- [8] M. Hitchman, F. Tian, Studies of TiO<sub>2</sub> thin films prepared by chemical vapour deposition for photocatalytic and photoelectrocatalytic degradation of 4-chlorophenol, *J. Electroanal. Chem.* 538-539 (2002) 165.
- [9] M. Uzunova, M. Kostadinov, J. Georgieva, C. Dushkin, D. Todorovsky, N. Philippidis, I. Poulios, S. Sotiropoulos, Photoelectrochemical characterisation and photocatalytic activity of composite La<sub>2</sub>O<sub>3</sub>-TiO<sub>2</sub> coatings on stainless steel, *Appl. Catal. B: Environ.* 73 (2007) 23.
- [10] R. van Grieken, J. Marugán, C. Sordo, C. Pablos, Comparison of the photocatalytic disinfection of *E. coli* suspensions in slurry, wall and fixed-bed reactors, *Catal. Today* 144 (2009) 48.
- [11] T. Nash, The colorimetric estimation of formaldehyde by means of the Hantzsch reaction, *Biochem. J.* 55 (1953) 416.
- [12] T.L. Villareal, R. Gómez, M. Neumann-Spallart, N. Alonso-Vante, P. Salvador,

Semiconductor photooxidation of pollutants dissolved in water: A kinetic model for distinguishing between direct and indirect interfacial hole transfer. I. Photolelectrochemical experiments with polycrystalline anatase electrodes under current doubling and absence of recombination, *J. Phys. Chem.* 108 (2004) 15172.

[13] L. Sun, J.R. Bolton, Determination of the quantum yield for the photochemical generation of hydroxyl radicals in TiO<sub>2</sub> suspensions. *J. Phys. Chem.* 100 (1996) 4127.

[14] A. Hamnett, Semiconductor Electrochemistry. *Compr. Chem. Kinet.* 27 (1987) 61.

[15] J. Byrne, B. Eggins, Photoelectrochemistry of oxalate on particulate TiO<sub>2</sub> electrodes, *J. Electroanal. Chem.* 457 (1998) 61.

[16] K. Rajeshwar, in: A. J. Bard, M. Stratmann (Eds.), *Encyclopedia of Electrochemistry*, Wiley-VCH, Darmstadt, 2002, p. 1.

[17] J. Georgieva, S. Armyanov, E. Valova, I. Poulios, S. Sotiropoulos, Preparation and photoelectrochemical characterisation of electrosynthesised titanium dioxide deposits on stainless steel substrates, *Electrochim. Acta.* 51 (2006) 2076.

[18] D. Jiang, H. Zhao, Z. Shanqing, R. John, Characterization of photoelectrocatalytic processes at nanoporous TiO<sub>2</sub> film electrodes: Photocatalytic oxidation of glucose, *Phys. Chem.* 107 (2003) 12774.

[19] Y. Ma, J. Qiu, Y. Cao, Z. Guan, J. Yao, Photocatalytic activity of TiO<sub>2</sub> films grown on different substrates, *Chemosphere.* 44 (2001) 1087.

[20] C. He, X.Z. Li, N. Graham, Y. Wang, Preparation of TiO<sub>2</sub>/ITO and TiO<sub>2</sub>/Ti photoelectrodes by magnetron sputtering for photocatalytic application, *Appl. Catal. A: Gen.* 305 (2006) 54.

[21] H. Zhao, D. Jiang, S. Zhang, W. Wen, Photoelectrocatalytic oxidation of organic compounds at nanoporous TiO<sub>2</sub> electrodes in a thin-layer photoelectrochemical cell, *J. Catal.* 250 (2007) 102.

[22] W. Leng, Z. Zhang, J. Zhang, Photoelectrocatalytic degradation of aniline over rutile TiO<sub>2</sub>/Ti electrode thermally formed at 600°C, *J. Mol. Catal. A: Chem.* 206 (2003) 239.

[23] I. Mintsaouli, N. Philippidis, I. Poulios, S. Sotiropoulos, Photoelectrochemical characterisation of thermal and particulate titanium dioxide electrodes, *J. Appl. Electrochem.* 36 (2006) 463.

- [24] G. Waldner, J. Krýsa, Photocurrents and degradation rates on particulate TiO<sub>2</sub> layers. Effect of layer thickness, concentration of oxidizable substance and illumination direction, *Electrochim. Acta*, 50 (2005) 4498.
- [25] X. Li, F. Li, C. Fan, Y. Sun, Photoelectrocatalytic degradation of humic acid in aqueous solution using a Ti/TiO<sub>2</sub> mesh photoelectrode, *Water Res.* 36 (2002) 2215.
- [26] J. Marugán, D. Hufschmidt, M. López-Muñoz, V. Selzer, D. Bahnemann, Photonic efficiency for methanol photooxidation and hydroxyl radical generation on silica-supported TiO<sub>2</sub> photocatalysts, *Appl. Catal. B: Environ.* 62 (2006) 201.
- [27] P. Christensen, T. Egerton, S. Kosa, J. Tinlin, K. Scott, The photoelectrocatalytic oxidation of aqueous nitrophenol using a novel reactor, *J. Appl. Electrochem.* 35 (2005) 683.
- [28] G. Waldner, M. Pourmodjib, R. Bauer, M. Neumann-Spallart, Photoelectrocatalytic degradation of 4-chlorophenol and oxalic acid on titanium dioxide electrodes, *Chemosphere*, 50 (2003) 989.
- [29] J. Rodríguez, M. Gómez, S. Lindquist, C. Granqvist, Photo-electrocatalytic degradation of 4-chlorophenol over sputter deposited Ti oxide films, *Thin Solid Films*, 360 (2000) 250.
- [30] W. Adams, M. Bakker, T. Quickenden, Photovoltaic properties of ordered mesoporous silica thin film electrodes encapsulating titanium dioxide particles, *J. Photoch. Photobiol. A: Chem.* 181 (2006) 166.
- [31] X. Cheng, W. Leng, D. Liu, Y. Xu, J. Zhang, C. Cao, Electrochemical preparation and characterization of surface-fluorinated TiO<sub>2</sub> nanoporous film and its enhanced photoelectrochemical and photocatalytic properties, *J. Phys. Chem. C* 112 (2008) 8725.
- [32] X. Song, J. M. Wu, M. Yan, Photocatalytic and photoelectrocatalytic degradation of aqueous Rhodamine B by low-temperature deposited anatase thin films, *Mater. Chem. Phys.* 112 (2008) 510.
- [33] W. Gan, M. Lee, R. Amal, H. Zhao, K. Chiang, Photoelectrocatalytic activity of mesoporous TiO<sub>2</sub> films prepared using the sol-gel method with tri-block copolymer as structure directing agent, *J. Appl. Electrochem.* 38 (2008) 703.
- [34] X.Z. Li, C. He, N. Graham, Y. Xiong, Photoelectrocatalytic degradation of bisphenol A in aqueous solution using a Au-TiO<sub>2</sub>/ITO film, *J. Appl. Electrochem.*, 35 (2005) 741.

[35] C. He, Y. Xiong, D. Shu, X. Zhu, X. Li, Preparation and photoelectrocatalytic activity of Pt(TiO<sub>2</sub>)-TiO<sub>2</sub> hybrid films, *Thin Solid Films*, 503 (2006) 1.

[36] M. Heikkilä, E. Puukilainen, M. Ritala, M. Leskelä, Effect of thickness of ALD grown TiO<sub>2</sub> films on photoelectrocatalysis, *J. Photochem. Photobiol. A: Chem.* 204 (2009) 200.